articles

molecular pharmaceutics

The Pharmacokinetics of Cell-Penetrating Peptides

Dikran Sarko,[†,‡] Barbro Beijer,[†] Regine Garcia Boy,[†] Eva-Maria Nothelfer,[†,§] Karin Leotta,[§] Michael Eisenhut,[||] Annette Altmann,[†,§] Uwe Haberkorn,[†,§] and Walter Mier*[,†]

Department of Nuclear Medicine, University Hospital Heidelberg, INF 400, 69120 Heidelberg, Germany, Faculty of Pharmacy, Al-Baath University, P.O. Box 77 Homs, Syria, Clinical Cooperation Unit Nuclear Medicine, DKFZ, INF 280, 69120 Heidelberg, Germany, and Department of Radiopharmaceutical Chemistry, DKFZ, INF 280, 69120 Heidelberg, Germany

Received July 2, 2010; Revised Manuscript Received September 13, 2010; Accepted September 16, 2010

Abstract: Cell-penetrating peptides (CPPs) are able to penetrate the cell membrane carrying cargoes such as peptides, proteins, oligonucleotides, siRNAs, radioisotopes, liposomes, and nanoparticles. Consequently, many delivery approaches have been developed to use CPPs as tools for drug delivery. However, until now a systematic analysis of their *in vivo* properties including potential tumor binding specificity for drug targeting purposes has not been conducted. Ten of the most commonly applied CPPs were obtained by solid phase peptide synthesis and labeled with ^{111}In or ^{68}Ga. Uptake studies were conducted using a panel of six tumor cell lines of different origin. The stability of the peptides was examined in human serum. Biodistribution experiments were conducted in nude mice bearing human prostate carcinoma. Finally, positron emission tomography (PET) measurements were performed in male Wistar rats. The *in vitro* uptake studies revealed high cellular uptake values, but no specificity toward any of the cell lines. The biodistribution in PC-3 tumor-bearing nude mice showed a high transient accumulation in well-perfused organs and a rapid clearance from the blood. All of the CPPs revealed a relatively low accumulation rate in the brain. The highest uptake values were observed in the liver (with a maximal uptake of 51 %ID/g observed for oligoarginine (R_9)) and the kidneys (with a maximal uptake of 94 %ID/g observed for NLS). The uptake values in the PC-3 tumor were low at all time points, indicating a lack of tumor specific accumulation for all peptides studied. A micro-PET imaging study with ^{68}Ga-labeled penetratin, Tat and transportan$_{10}$ (TP_{10}) confirmed the organ distribution data. These data reveal that CPPs do not show evidence for application in tumor targeting purposes *in vivo*. However, CPPs readily penetrate into most organs and show rapid clearance from the circulation. The high uptake rates observed *in vitro* and the relatively low specificity *in vivo* imply that CPPs would be better suited for topical application in combination with cargoes which show passive targeting and dominate the pharmacokinetic behavior. In conclusion, CPPs are suitable as drug carriers for *in vivo* application provided that their pharmacokinetic properties are also considered in design of CPP drug delivery systems.

Keywords: Tumor targeting; cell-penetrating peptides; pharmacokinetics; biodistribution; serum stability; peptide tracers; positron emission tomography

Introduction

The achievements in the field of molecular medicine provide fascinating alternatives to common therapeutic strategies. However, the application of novel biological therapeutics based on molecular medicine knowledge is often complicated by the large size of these compounds. Most tracers with a pronounced specificity (e.g., antibodies) possess a high molecular weight—obviously an intrinsic property of highly selective drugs—which results in unfavor-

* Corresponding author. Mailing address: University Hospital Heidelberg, Department of Nuclear Medicine, Im Neuenheimer Feld 400, D-69120 Heidelberg, Germany. Tel: +49-6221-567720. Fax: +49-6221-5633629. E-mail: walter.mier@med.uni-heidelberg.de.

† University Hospital Heidelberg.

‡ Al-Baath University.

§ Clinical Cooperation Unit Nuclear Medicine, DKFZ.

|| Department of Radiopharmaceutical Chemistry, DKFZ.

10.1021/mp100223d
Published on Web 09/16/2010

Figure 1. Chemical structure of the compounds studied as exemplified for ^{111}In-DOTA-penetratin.

able pharmacokinetic qualities setting hurdles for their clinical application. The successful clinical application of many high molecular weight drugs is hampered by their inability to efficiently traverse the cellular plasma membrane.

In the early 1990s, it was discovered that the third helix of the homeodomain of *Drosophila Antennapedia* (amino acids 43−58) translocates through biological membranes. This peptide was referred to as penetratin.[1] Thereafter, other peptides were reported to act in a similar way to penetratin and this new class of peptides was named cell-penetrating peptides (CPPs).[1−5] CPPs are relatively short peptides of 5−40 amino acids in length with the ability to gain access to the cell interior by means of different mechanisms, including endocytosis, with the capacity to promote the intracellular delivery of covalently or noncovalently conjugated bioactive cargoes.[6] However, there is a lack of information about the pharmacological properties of these molecules when applied *in vivo*.

CPPs may provide a solution to the previously mentioned problem as they are able to cross the plasma membrane carrying large drugs including peptides, proteins, oligonucleotides, siRNAs, radioisotopes, liposomes, hormones, and nanoparticles.[7−20] The size of the cargoes can exceed the CPPs' vector size by several fold. Consequently, CPPs have emerged as a promising tool in drug delivery.

Unfortunately, most of the previous studies were limited to the evaluation of only two or three CPPs,[21] or to *in vitro* applications.[22] In addition to the internalization mechanism of CPPs, information on the stability and pharmacokinetic properties of CPPs *in vivo* is of significance for clinical applications. Few researchers have attempted to link CPPs with labels for computed tomography (CT) and/or magnetic resonance imaging (MRI).[23,24] Tagging of CPPs for molecular imaging may reveal information on their utility for *in vivo* applications i.e. to target specific organs, the blood clearance or the permeability of the blood brain barrier (BBB).

To assess the potential of CPPs for *in vivo* targeting purposes, ten of the most commonly used CPPs were investigated *in vitro* as well as *in vivo*.[25] The peptides were obtained by solid phase synthesis, conjugated to the chelator DOTA and radiolabeled using ^{111}In or ^{68}Ga (see Figure 1). This minimal modification was chosen to avoid eventual influences of the molecular size on functional affinity. The stability in human serum was determined, the cellular uptake was studied in six tumor cell lines of different origin and the *in vivo* biodistribution was studied in PC-3 tumor-bearing mice. These biodistribution data were confirmed by micro-PET imaging.

Materials and Methods

Peptide Synthesis. The peptides were synthesized by solid phase peptide synthesis using fluorenylmethyloxycarbonyl (Fmoc) chemistry. Tris-^{t}Bu-DOTA (tris-^{t}Bu-1,4,7,10-tetraazacyclododecane-1,4,7,10-tetraacetic acid) was used to obtain DOTA-conjugated peptides. The peptides were purified and analyzed by reverse-phase high-performance liquid

(1) Derossi, D.; Joliot, A. H.; Chassaing, G.; Prochiantz, A. The Third Helix of the *Antennapedia* Homeodomain Translocates Through Biological Membranes. *J. Biol. Chem.* **1994**, *269*, 10444–104450.
(2) Vives, E.; Brodin, P.; Lebleu, B. A Truncated HIV-1 Tat Protein Basic Domain Rapidly Translocates Through the Plasma Membrane and Accumulates in the Cell Nucleus. *J. Biol. Chem.* **1997**, *272*, 16010–16017.
(3) Mitchell, D. J.; Kim, D. T.; Steinman, L.; Fathman, C. G.; Rothbard, J. B. Polyarginine Enters Cells More Efficiently Than Other Polycationic Homopolymers. *J. Pept. Res.* **2000**, *56*, 318–325.
(4) Oehlke, J.; Scheller, A.; Wiesner, B.; Krause, E.; Beyermann, M.; Klauschenz, E.; Melzig, M.; Bienert, M. Cellular Uptake of an Alpha-Helical Amphipathic Model Peptide with the Potential to Deliver Polar Compounds into the Cell Interior Non-Endocytically. *Biochim. Biophys. Acta* **1998**, *1414*, 127–139.
(5) Soomets, U.; Lindgren, M.; Gallet, X.; Hallbrink, M.; Elmquist, A.; Balaspiri, L.; Zorko, M.; Pooga, M.; Brasseur, R.; Langel, U. Deletion Analogues of Transportan. *Biochim. Biophys. Acta* **2000**, *1467*, 165–176.
(6) *Handbook of Cell-Penetrating Peptides*, 2nd ed.; Langel, U., Ed.; CRC Press: Boca Raton, 2007.
(7) Wang, J.; Lu, Z.; Wientjes, M. G.; Au, J. L. Delivery of siRNA Therapeutics: Barriers and Carriers. *AAPS J.* **2010**. doi: 10.1208/s12248-010-9210-4.
(8) Bertrand, J. R.; Malvy, C.; Auguste, T.; Toth, G. K.; Kiss-Ivankovits, O.; Illyes, E.; Hollosi, M.; Bottka, S.; Laczko, I. Synthesis and Studies on Cell-Penetrating Peptides. *Bioconjugate Chem.* **2009**, *20*, 1307–1314.
(9) Bitler, B. G.; Schroeder, J. A. Anti-Cancer Therapies That Utilize Cell Penetrating Peptides. *Recent Pat. Anti-Cancer Drug Discovery* **2010**, *5*, 99–108.
(10) Said Hassane, F.; Saleh, A.; Abes, R.; Gait, M.; Lebleu, B. Cell Penetrating Peptides: Overview and Applications to the Delivery of Oligonucleotides. *Cell. Mol. Life Sci.* **2010**, *67*, 715–726.
(11) Brooks, N. A.; Pouniotis, D. S.; Tang, C.-K.; Apostolopoulos, V.; Pietersz, G. A. Cell-Penetrating Peptides: Application in Vaccine Delivery. *Biochim. Biophys. Acta, Rev. Cancer* **2010**, *1805*, 25–34.
(12) Fretz, M. M.; Storm, G. TAT-Peptide Modified Liposomes: Preparation, Characterization, and Cellular Interaction. *Methods Mol. Biol.* **2010**, *605*, 349–359.
(13) Olson, E. S.; Jiang, T.; Aguilera, T. A.; Nguyen, Q. T.; Ellies, L. G.; Scadeng, M.; Tsien, R. Y. Activatable Cell Penetrating Peptides Linked to Nanoparticles as Dual Probes for *in vivo* Fluorescence and MR Imaging of Proteases. *Proc. Natl. Acad. Sci. U.S.A.* **2010**, *107*, 4311–4316.

chromatography (RP-HPLC) and characterized by matrix-assisted laser desorption ionization time-of-flight (MALDI-TOF) mass spectrometry.

Peptide Labeling. 5 μL of a 10^{-3} M solution of the respective peptide in 4 M sodium acetate buffer (pH 5) and 10−50 MBq of either ^{68}Ga (eluted from a ^{68}Ge/^{68}Ga generator[26]) or $^{111}InCl_3$ (Perkin-Elmer, USA) were heated in a total volume of 50 μL at 95 °C for 10 min. Radio-HPLC on a monolithic RP-HPLC column 100 × 4.6 mm column (Merck, Darmstadt, Germany) using 0.1% trifluoroacetic acid (TFA) in water and 0.1% TFA in acetonitrile as eluents showed yields >95%.

Stability Determination. 2−4 MBq of the ^{111}In-labeled CPPs were mixed with 500 μL of human serum, freshly prepared from healthy volunteers and incubated at 37 °C. Samples were taken after 0, 2, 5, 10, 30, 60, 120, 240, 480, and 1440 min incubation and mixed with a 2-fold excess of acetonitrile to precipitate serum proteins. The suspension was incubated at 4 °C for 1 h and centrifuged for 5 min at 13,000 rpm. The supernatant containing the peptide was analyzed by radio-HPLC as described above.

Cell Lines. All cell lines were cultivated at 37 °C in a 5% CO_2 incubator. The human anaplastic thyroid carcinoma cell line SW1736 (obtained from N.E. Heldin, Uppsala, Sweden), the human prostate cancer cell line PC-3 (ATCC, Manassas, VA), and the human colorectal carcinoma cell line HCT-116 (ATCC, Manassas, VA) were cultured in RPMI 1640 with Glutamax, containing 10% fetal calf serum (Invitrogen Karlsruhe, Germany) and 25 mM HEPES. MH3924A Morris hepatoma cells were cultured in RPMI 1640 (with 1% L-glutamine, 10% fetal calf serum (FCS) and 2.0 g/L $NaHCO_3$) and DPBS buffer (Pan Biotech GmbH, Aidenbach, Germany). The human breast cancer cell line MCF 7 and the human squamous cell carcinoma cell line HNO 97 (obtained from Dr. Herold-Mende, University Hospital Heidelberg, Germany) were cultured in DMEM with Glutamax, containing 10% fetal calf serum (Invitrogen Karlsruhe, Germany) and 25 mM HEPES.

***In Vitro* Binding Experiments.** 300,000 cells were seeded into 6-well plates and cultivated for 24 h. The medium was replaced by 1 mL of fresh medium (without FCS) preheated to 37 °C. The ^{111}In-labeled peptide was added to the cell culture (1.5−2 × 10^6 cpm/well) and incubated at 37 °C for 30 min or 3 h. The cells were washed three times with 1 mL of phosphate-buffered saline and subsequently lysed with 0.5 mL of 0.3 M NaOH. Radioactivity was determined in a γ counter and calculated as percent of the applied dose per 10^6 cells.

Animals and Tumor Growth. 5 × 10^6 cells of the prostate carcinoma cell line PC-3 were subcutaneously inoculated into the anterior region of the trunk of 6-week-old female nu/nu mice (Charles River WIGA, Sulzfeld, Germany). The studies were started 10−14 days after tumor inoculation, when the tumors had reached a size of approximately 1 cm^3. All animals were cared for and treated according to the national animal guidelines.

Biodistribution Studies of the ^{111}In-Labeled DOTA−CPPs. Biodistribution studies of the different CPPs were performed in mice to analyze their tissue selectivity, blood persistence, body clearance and potential tumor localization. 100 μL of a 0.5−1 MBq solution of the radiolabeled peptide was injected via the tail vein of the PC-3 prostate tumor-bearing mice. After 10, 60 or 240 min p.i. the animals were sacrificed. Blood, heart, lung, spleen, liver, kidney, muscle, intestine, brain and the tumors were dissected, blotted dry and weighed. The radioactivity was measured in a γ counter (Cobra II, Canberra Packard, Meriden, USA) along with a

(14) Patel, L. N.; Wang, J.; Kim, K. J.; Borok, Z.; Crandall, E. D.; Shen, W. C. Conjugation with Cationic Cell-Penetrating Peptide Increases Pulmonary Absorption of Insulin. *Mol. Pharmaceutics* **2009**, *6*, 492–503.
(15) Yvonne, T.; Gerd, W.; Pille, S.; Burkhard, W.; Stephan, P.; Johannes, O. Cellular Uptake and Biological Activity of Peptide Nucleic Acids Conjugated with Peptides with and without Cell-Penetrating Ability. *J. Pept. Sci.* **2010**, *16*, 71–80.
(16) Liu, Y.; Ibricevic, A.; Cohen, J. A.; Cohen, J. L.; Gunsten, S. P.; Frechet, J. M. J.; Walter, M. J.; Welch, M. J.; Brody, S. L. Impact of Hydrogel Nanoparticle Size and Functionalization on *in vivo* Behavior for Lung Imaging and Therapeutics. *Mol. Pharmaceutics* **2009**, *6*, 1891–1902.
(17) Peetla, C.; Stine, A.; Labhasetwar, V. Biophysical Interactions with Model Lipid Membranes: Applications in Drug Discovery and Drug Delivery. *Mol. Pharmaceutics* **2009**, *6*, 1264–1276.
(18) Zhang, X.; Jin, Y.; Plummer, M. R.; Pooyan, S.; Gunaseelan, S.; Sinko, P. J. Endocytosis and Membrane Potential Are Required for HeLa Cell Uptake of R.I.-CKTat9, a Retro-Inverso Tat Cell Penetrating Peptide. *Mol. Pharmaceutics* **2009**, *6*, 836–848.
(19) Peetla, C.; Rao, K. S.; Labhasetwar, V. Relevance of Biophysical Interactions of Nanoparticles with a Model Membrane in Predicting Cellular Uptake: Study with TAT Peptide-Conjugated Nanoparticles. *Mol. Pharmaceutics* **2009**, *6*, 1311–1320.
(20) Zaro, J. L.; Vekich, J. E.; Tran, T.; Shen, W.-C. Nuclear Localization of Cell-Penetrating Peptides Is Dependent on Endocytosis Rather Than Cytosolic Delivery in CHO Cells. *Mol. Pharmaceutics* **2009**, *6*, 337–344.
(21) Amantana, A.; Moulton, H. M.; Cate, M. L.; Reddy, M. T.; Whitehead, T.; Hassinger, J. N.; Youngblood, D. S.; Iversen, P. L. Pharmacokinetics, Biodistribution, Stability and Toxicity of a Cell-Penetrating Peptide-Morpholino Oligomer Conjugate. *Bioconjugate Chem.* **2007**, *18*, 1325–1331.
(22) Mueller, J.; Kretzschmar, I.; Volkmer, R.; Boisguerin, P. Comparison of Cellular Uptake Using 22 CPPs in 4 Different Cell Lines. *Bioconjugate Chem.* **2008**, *19*, 2363–2374.
(23) Liu, M.; Guo, Y. M.; Yang, J. L.; Wang, P.; Zhao, L. Y.; Shen, N.; Wang, S. C.; Guo, X. J.; Wu, Q. F. Application of Cell Penetrating Peptide in Magnetic Resonance Imaging of Bone Marrow Mesenchymal Stem Cells. *Acta Biochim. Biophys. Sin.* **2006**, *38*, 865–873.
(24) Guo, Y. M.; Liu, M.; Yang, J. L.; Guo, X. J.; Wang, S. C.; Duan, X. Y.; Wang, P. Intercellular Imaging by a Polyarginine Derived Cell Penetrating Peptide Labeled Magnetic Resonance Contrast Agent, Diethylenetriamine Pentaacetic Acid Gadolinium. *Chin. Med. J.* **2007**, *120*, 50–55.
(25) Fischer, R.; Fotin-Mleczek, M.; Hufnagel, H.; Brock, R. Break on Through to the Other Side-Biophysics and Cell Biology Shed Light on Cell-Penetrating Peptides. *ChemBioChem* **2005**, *6*, 2126–2142.
(26) Schuhmacher, J.; Maier-Borst, W. A New 68Ge/^{68}Ga Radioisotope Generator System for Production of 68Ga in Dilute HCl. *Int. J. Appl. Radiat. Isot.* **1981**, *32*, 31–36.

Table 1. Sequences of the DOTA-conjugated CPPs and their Half-lives in Human Serum

peptide	sequence	$t_{1/2}$ (h)	refs
penetratin	DOTA-RQIKIWFQNRRMKWKK	1.2	1
Tat	DOTA-GRKKRRQRRRPPQ	8.8	2
$PreS_2$-TLM	DOTA-PLSSIFSRIGDP	4.4	27
MAP[a]	DOTA-KLALKLALKALKAALKLA	>72	4
R_9[b]	DOTA-RRRRRRRRR	1.9	3
pVEC	DOTA-LLIILRRRIRKQAHAHSK	3.9	28
MTS[c]	DOTA-AAVALLPAVLLALLAP	48.1	29
$SynB_1$	DOTA-RGGRLSYSRRRFSTSTGR	5.2	30
TP_{10}[d]	AGYLLGKϵ(DOTA)INLKALAALAKKIL	>72	5
NLS[e]	PKKKRKVKϵ(DOTA)	>72	31

[a] Model amphipathic peptide. [b] Oligoarginine. [c] Membrane translocating sequence of k-FGF. [d] $Transportan_{10}$. [e] Nuclear Localization Signal (SV 40).

sample of the injection solution to calculate the percentage of injected dose per gram of tissue (%ID/g).

PET. Male Wistar rats (480−550 g) were anesthetized using isofluorane inhalation and injected with 75−135 MBq of the respective ^{68}Ga-labeled CPP. Subsequent imaging was performed on an Inveon small-animal PET scanner (Siemens) using a 60 min emission scan in the list mode and a 10 min transmission scan. Images were taken in the 3-dimensional (3D) mode and reconstructed iteratively with a fully 3D algorithm from a 256 × 256 matrix for viewing transaxial, coronal, and sagittal slices of 0.9 mm thickness. Pixel size was 0.38 × 0.38 × 0.79 mm, and transaxial resolution obtained was 0.9 mm.

Results

Peptide Synthesis and Labeling. The DOTA-conjugated peptides were synthesized by solid-phase peptide synthesis (SPPS) using Fmoc chemistry and 2-(1*H*-benzotriazol-1-yl)-1,1,3,3-tetramethyluroniumhexafluorophosphate (HBTU)/diisopropylethylamine activation. The peptides synthesized are listed in Table 1.

The peptides were purified, analyzed by RP-HPLC and characterized using MALDI-TOF mass spectrometry.

Serum Stability of ^{111}In-DOTA−CPPs. The stability of the ^{111}In-DOTA−CPPs in human serum was determined by radio-HPLC analysis of samples taken after 0, 2, 5, 10, 30, 60, 120, 240, 480, and 1440 min. In the case of the peptides MAP, R_9 and pVEC, a high fraction of the radioactivity (up to 89%) was associated with the proteins precipitated, which complicated the analysis. These results support the fact that the oligoarginine peptides are adsorbed to the serum proteins.[32] The half-life values ($t_{1/2}$) of the peptide conjugates were calculated under the assumption of an exponential degradation. The results are shown in Table 1.

***In Vitro* Binding Experiments.** The cellular uptake of the ^{111}In-labeled peptide conjugates was studied in a series of tumor cell lines of different origin after incubation for 30 and 180 min. The specific accumulation in the different cells is summarized in Table 2.

Although all the CPPs studied are supposed to have cell-penetrating properties, they do not show the same efficiency of cellular uptake. By taking the average of the cellular uptake of all ^{111}In-labeled peptides in all six different tumor cell lines; three groups of CPPs were discriminated depending on their cellular uptake efficiency.[22] The first group (>80% applied dose in 10^6 cells) includes penetratin and MAP. The second group (between 10−80% applied dose in 10^6 cells) includes Tat, pVEC, $SynB_1$ and $transportan_{10}$. The third group comprises the CPPs with a cellular uptake efficiency lower than 10% applied dose in 10^6 cells including $PreS_2$-TLM, R_9, MTS, and NLS. The accumulation was found to be rapid: in general, higher uptake values were observed after 30 min than after 180 min.

In a comparison of all cell lines tested, the SW 1736 cell line shows the highest accumulation rate (224% applied dose/10^6 cells after 30 min in the case of peptide MAP), and the HCT 116 cell line shows the lowest rate (0.11% applied dose/10^6 cells after 30 min in the case of peptide $PreS_2$-TLM).

Biodistribution of Radiolabeled CPPs. The distribution of the ^{111}In-labeled CPPs after i.v. injection in PC-3 tumor-bearing mice is shown in Tables 3−5 as the percentage of the injected dose per gram tissue (%ID/g). All of the radiolabeled CPPs showed a relatively fast blood clearance with %ID/g values decreasing to less than 1 %ID/g after 4 h. In general, the tumor showed the lowest uptake rates among all organs (except for the brain and muscles) for all of the peptides studied. Noticeable values were observed for R_9 with 51.4 %ID/g in the liver 10 min after injection, and a rapid accumulation of 81.4 %ID/g in the kidneys was observed for NLS just after 10 min. Penetratin was found to cross the blood brain barrier within 10 min at a level of 0.9 %ID/g in the brain indicating a distinct blood brain barrier permeability of CPPs. After 4 h, all of the peptides (except

(27) Oess, S.; Hildt, E. Novel Cell Permeable Motif Derived from the $PreS_2$-Domain of Hepatitis-B Virus Surface Antigens. *Gene Ther.* **2000**, *7*, 750–758.
(28) Elmquist, A.; Lindgren, M.; Bartfai, T.; Langel, U. VE-Cadherin-Derived Cell-Benetrating Peptide, pVEC, with Carrier Functions. *Exp. Cell Res.* **2001**, *269*, 237–244.
(29) Lin, Y. Z.; Yao, S. Y.; Veach, R. A.; Torgerson, T. R.; Hawiger, J. Inhibition of Nuclear Translocation of Transcription Factor NF-Kappa B by a Synthetic Peptide Containing a Cell Membrane-Permeable Motif and Nuclear Localization Sequence. *J. Biol. Chem.* **1995**, *270*, 14255–14258.
(30) Rousselle, C.; Clair, P.; Lefauconnier, J. M.; Kaczorek, M.; Scherrmann, J. M.; Temsamani, J. New Advances in the Transport of Doxorubicin through the Blood-Brain Barrier by a Peptide Vector-Mediated Strategy. *Mol. Pharmacol.* **2000**, *57*, 679–686.
(31) Kalderon, D.; Roberts, B. L.; Richardson, W. D.; Smith, A. E. A Short Amino Acid Sequence Able to Specify Nuclear Location. *Cell* **1984**, *39*, 499–509.
(32) Kosuge, M.; Takeuchi, T.; Nakase, I.; Jones, A. T.; Futaki, S. Cellular Internalization and Distribution of Arginine-Rich Peptides as a Function of Extracellular Peptide Concentration, Serum, and Plasma Membrane Associated Proteoglycans. *Bioconjugate Chem.* **2008**, *19*, 656–664.

Table 2. Cellular Uptake Values of the Peptide Conjugates in Different Cell Lines

		percentage of the applied dose per 10^6 cells					
peptide	time (min)	SW 1736	PC-3	MH wt	HNO 97	MCF- 7	HCT 116
penetratin	30	186.6 ± 41.5	88 ± 11.5	42 ± 3	76.4 ± 19.9	59.9 ± 2.4	21.1 ± 2.5
	180	111.6 ± 6.5	60.7 ± 2.6	19.9 ± 3.5	89.3 ± 7.4	44.1 ± 3.1	16.9 ± 1
Tat	30	105.6 ± 3.4	57.6 ± 23.1	31.4 ± 4.6	53.8 ± 6.3	19.2 ± 1.8	12.5 ± 3.3
	180	31.4 ± 14.1	15.2 ± 3.5	11.5 ± 5.1	44.8 ± 11.8	2.5 ± 1.2	2.4 ± 0.2
$PreS_2$-TLM	30	0.3 ± 0	4.3 ± 0.3	0.1 ± 0	0.1 ± 0	2.1 ± 0.8	0.1 ± 0
	180	0.2 ± 0	25.6 ± 2.6	0.3 ± 0.3	0.1 ± 0	21.8 ± 2.2	0 ± 0
MAP	30	224.1 ± 30.6	64.9 ± 19.8	70.4 ± 34.5	69.3 ± 9.8	103.5 ± 17.5	25.4 ± 2.2
	180	133.9 ± 23.4	60.6 ± 14.5	43.4 ± 5.7	79.5 ± 7.5	83.9 ± 12.2	18.2 ± 1.5
R_9	30	8.1 ± 1.6	6.9 ± 0.7	3.4 ± 0.7	4.5 ± 2.5	5.2 ± 1	2.1 ± 0.2
	180	4.7 ± 1.6	5 ± 2.4	1.1 ± 0.2	3 ± 1.1	2.8 ± 0.2	0.9 ± 0.2
pVEC	30	90.4 ± 7.9	44.5 ± 4.1	20.6 ± 1.1	3.5 ± 0.6	17.7 ± 1.3	12.3 ± 0.6
	180	65.6 ± 5.1	39.4 ± 3.4	2.3 ± 0.4	10.8 ± 1.4	17.6 ± 0.6	7.4 ± 0.4
MTS	30	20.6 ± 10.6	5.7 ± 0.6	0.9 ± 0.2	7.5 ± 2	14.1 ± 1.1	2.9 ± 0.5
	180	10 ± 2.9	4.3 ± 0.9	0.4 ± 0.2	10.4 ± 4.1	8.6 ± 2.4	2.2 ± 0.5
$SynB_1$	30	105.1 ± 5.9	30.8 ± 4.3	15.3 ± 0.6	4.5 ± 0.7	13.9 ± 0.1	9.3 ± 0.4
	180	55.5 ± 1.9	8 ± 1	0.6 ± 0.1	31.6 ± 1.8	4.4 ± 0	4.9 ± 0.1
TP_{10}	30	72.6 ± 22.8	16.3 ± 5.3	2.9 ± 1.5	32.8 ± 14.9	102.6 ± 34.5	23.5 ± 6.6
	180	60.7 ± 10.3	15 ± 2.7	2.8 ± 0.6	52.1 ± 13.9	101.3 ± 16.4	10.5 ± 4.5
NLS	30	3.3 ± 0.2	2.1 ± 0.1	0.7 ± 0.1	0.3 ± 0.1	0.6 ± 0	0.4 ± 0
	180	2.9 ± 0.2	8.3 ± 3.7	0.3 ± 0	0.3 ± 0.1	5.4 ± 0.4	0.3 ± 0

Table 3. Biodistribution of the ^{111}In-Labeled CPPs at 10 min Postinjection into 6-Week-Old nu/nu Female Mice Bearing PC-3 Tumors (Average %ID/g ± Standard Deviation) ($n = 3$)

peptide	blood	heart	lung	spleen	liver	kidney	muscle	intestine	brain	tumor
penetratin	3.4 ± 0.4	2.3 ± 0.3	5.7 ± 0.8	10.2 ± 3.6	23.6 ± 3.1	25.5 ± 4.4	1.9 ± 0.3	2.6 ± 0.5	0.9 ± 1.1	2.5 ± 0.3
Tat	5.9 ± 1.4	6.5 ± 0.8	12.6 ± 1.6	9.5 ± 3.4	16.7 ± 2.1	43.9 ± 5.8	2.6 ± 0.2	7 ± 1.7	0.4 ± 0.1	3.6 ± 0.7
$PreS_2$-TLM	3.8 ± 0.4	1.5 ± 0.3	3 ± 0.4	0.9 ± 0.1	1.5 ± 0.3	11.6 ± 3.1	0.9 ± 0.2	1.1 ± 0.2	0.3 ± 0.2	2.2 ± 0
MAP	7.2 ± 1.1	3.7 ± 0.6	4.7 ± 0.6	5.8 ± 2.3	23.6 ± 6.6	18.7 ± 4.1	1.2 ± 0.1	2.2 ± 0.2	0.3 ± 0.1	1.6 ± 0.2
R_9	3.1 ± 0.8	2.4 ± 0.8	4.6 ± 1	12.1 ± 2.5	51.4 ± 2.9	15.9 ± 2.1	1.5 ± 0.1	2.4 ± 0.4	0.2 ± 0	1.3 ± 0.3
pVEC	3.9 ± 0.9	2.2 ± 0.2	5.6 ± 0.3	7 ± 1.9	37.9 ± 6.1	44 ± 7.6	1.3 ± 0	2.6 ± 0.2	0.3 ± 0	2.9 ± 0.7
MTS	2.9 ± 0.7	1 ± 0.2	1.8 ± 0.3	1 ± 0.2	33.8 ± 3.5	4.7 ± 1.8	0.6 ± 0.1	0.7 ± 0.1	0.2 ± 0	0.9 ± 0.2
$SynB_1$	5.7 ± 0.7	2.4 ± 0.2	5.7 ± 0.7	4.2 ± 1.2	16.8 ± 1.6	36 ± 4.1	1.7 ± 0.2	2.4 ± 0.2	0.3 ± 0	3.2 ± 0.7
TP_{10}	3.8 ± 0.6	1.6 ± 0.5	2.4 ± 0.3	5 ± 1	20.2 ± 4.1	15.3 ± 1.5	0.7 ± 0.1	2 ± 0.4	0.2 ± 0.1	1 ± 0.1
NLS	4.8 ± 1.3	2 ± 0.6	5.1 ± 1.5	1.8 ± 0.6	2.8 ± 0.7	81.4 ± 3	2 ± 1.1	1.6 ± 0.3	0.4 ± 0.1	3.3 ± 1

Table 4. Biodistribution of the ^{111}In-Labeled CPPs at 1 h Postinjection into 6 Week Old nu/nu Female Mice Bearing PC-3 Tumors (Average %ID/g ± Standard Deviation) ($n = 3$)

peptide	blood	heart	lung	spleen	liver	kidney	muscle	intestine	brain	tumor
penetratin	0.8 ± 0.3	0.9 ± 0.1	1.9 ± 0.5	10.7 ± 2.1	25.6 ± 0.9	22.6 ± 2.5	0.7 ± 0.1	1.5 ± 0.1	0.1 ± 0	1 ± 0.2
Tat	1.1 ± 0.2	0.7 ± 0.1	2 ± 0.5	1.9 ± 0.3	11.8 ± 1.3	66.5 ± 9.5	0.7 ± 0.1	0.8 ± 0	0.1 ± 0	0.8 ± 0.2
$PreS_2$-TLM	0.2 ± 0.2	0.1 ± 0	0.1 ± 0.1	0.1 ± 0	0.2 ± 0	1.4 ± 0.2	0.2 ± 0.1	0.1 ± 0	0.1 ± 0	0.5 ± 0.5
MAP	0.5 ± 0.1	1 ± 0.1	1.2 ± 0.2	4.6 ± 1.1	21.1 ± 3	13.4 ± 2.9	0.6 ± 0.2	1.5 ± 0.2	0.1 ± 0	0.7 ± 0.1
R_9	0.6 ± 0.3	0.5 ± 0.1	1.4 ± 0.4	8.2 ± 3	49.9 ± 2.6	8.1 ± 1.1	0.6 ± 0.2	0.4 ± 0.1	0.1 ± 0	0.4 ± 0.1
pVEC	0.7 ± 0.1	0.6 ± 0	1.6 ± 0.1	5 ± 1.6	28.9 ± 5.9	32.8 ± 5.4	0.6 ± 0.1	1.3 ± 0.3	0.1 ± 0	1.3 ± 0.2
MTS	1.6 ± 0.7	0.6 ± 0.3	1 ± 0.3	0.7 ± 0	25.5 ± 4.2	4 ± 0.9	0.5 ± 0.2	0.5 ± 0.2	0.1 ± 0	0.6 ± 0.3
$SynB_1$	0.6 ± 0.3	0.4 ± 0.1	0.7 ± 0.1	1.7 ± 0.4	12.6 ± 2.3	22.3 ± 2.4	0.4 ± 0.1	0.3 ± 0.1	0.1 ± 0	0.7 ± 0.2
TP_{10}	0.4 ± 0.2	0.4 ± 0.1	0.8 ± 0.5	2.8 ± 0.4	14.5 ± 1.3	5.8 ± 0.7	0.3 ± 0.1	1.9 ± 0.9	0.1 ± 0	0.5 ± 0.2
NLS	0.9 ± 0.1	0.5 ± 0.1	2.1 ± 0.6	0.9 ± 0.1	1.7 ± 0.3	94 ± 7.4	1 ± 0.8	0.6 ± 0.3	0.2 ± 0.1	0.6 ± 0.1

for $PreS_2$-TLM) were retained in the liver and the kidneys. A high spleen uptake was observed after 4 h for both penetratin and R_9 (7.1 %ID/g and 9.1 %ID/g, respectively).

PET. Since only a low tumor uptake was observed in the biodistribution studies, additional PET studies were performed in non-tumor-bearing Wistar rats. PET images of the

Table 5. Biodistribution of the ^{111}In-Labeled CPPs at 4 h Postinjection into 6 Week Old nu/nu Female Mice Bearing PC-3 Tumors (Average %ID/g ± Standard Deviation) ($n = 3$)

peptide	blood	heart	lung	spleen	liver	kidney	muscle	intestine	brain	tumor
penetratin	0.6 ± 0.3	0.7 ± 0.2	1.6 ± 0.7	7.1 ± 3.2	29.2 ± 7.3	24.2 ± 4	0.8 ± 0.1	1.2 ± 0.2	0.1 ± 0	0.7 ± 0.2
Tat	0.1 ± 0.1	0.2 ± 0	0.3 ± 0	1.3 ± 0.4	10.2 ± 0.6	55.4 ± 6.8	0.5 ± 0.5	0.4 ± 0.1	0.1 ± 0.1	0.2 ± 0
$PreS_2$-TLM	0.1 ± 0	0.1 ± 0	0.1 ± 0	0.1 ± 0	0.1 ± 0	1.2 ± 0.2	0.1 ± 0.1	0.1 ± 0.1	0.2 ± 0.1	0.1 ± 0
MAP	0.1 ± 0	0.5 ± 0.1	0.5 ± 0.2	2.6 ± 0.7	16.2 ± 5	10.7 ± 1.4	0.3 ± 0	0.8 ± 0.3	0 ± 0	0.4 ± 0.1
R_9	0.5 ± 0.1	0.8 ± 0.2	0.9 ± 0.2	9.1 ± 0.5	54.4 ± 7.7	8.2 ± 2.5	0.9 ± 0.2	0.3 ± 0	0.1 ± 0	0.2 ± 0
pVEC	0.2 ± 0.2	0.3 ± 0.2	0.9 ± 0.5	3.1 ± 2.2	23.8 ± 16.8	34.1 ± 23.9	0.6 ± 0.4	0.8 ± 0.5	0.1 ± 0	0.8 ± 0.4
MTS	0.4 ± 0	0.2 ± 0	0.3 ± 0	0.5 ± 0.1	8.4 ± 6.6	2.1 ± 0.3	0.1 ± 0	0.2 ± 0	0 ± 0	0.2 ± 0
$SynB_1$	0.1 ± 0	0.2 ± 0	0.3 ± 0	2 ± 0.4	12.1 ± 1.6	21.5 ± 3.7	0.2 ± 0.1	0.2 ± 0.1	0.1 ± 0	0.2 ± 0
TP_{10}	0.1 ± 0	0.3 ± 0	0.3 ± 0	2.7 ± 0.8	14 ± 3.2	5.2 ± 0.4	0.2 ± 0	0.8 ± 0	0 ± 0	0.2 ± 0.1
NLS	0.4 ± 0	0.2 ± 0	0.8 ± 0.2	0.8 ± 0.1	1.2 ± 0.1	88.3 ± 17.9	0.5 ± 0.1	0.7 ± 0.7	0.1 ± 0	0.3 ± 0

^{68}Ga-labeled peptides penetratin, Tat, and TP_{10} were obtained 1 h after intravenous injection. The results are presented in Figure 2. The tomographic images confirmed the results obtained in the biodistribution studies. The rapid excretion of the three CPPs results in a low activity background in the abdomen, the lungs, the muscles and the circulation. The liver and the kidneys are the primary organs of peptide accumulation in the case of penetratin and Tat. The broader accumulation of TP_{10}, which includes the blood vessels, the heart and the spleen, revealed a significantly longer circulation time of this peptide.

In order to study the penetration of the blood brain barrier by Tat, an eventual accumulation in the brain was determined. The results obtained for the accumulation of the ^{68}Ga-labeled Tat are presented in Figure 3. These images reveal that the peptide is not taken up into the brain in significant amounts.

Discussion

The achievements in the field of molecular medicine provide fascinating alternatives to commonly applied treatment strategies. However, the application of novel biological therapeutics, based on molecular medicine knowledge are often complicated by the large size of these compounds. CPPs may provide a solution to the above-mentioned problem as they are able to cross the plasma membrane carrying large drugs including peptides, proteins, oligonucleotides, siRNAs, radioisotopes, liposomes, hormones, and nanoparticles. The size of the cargoes can exceed the CPPs' vector size by several fold. Consequently, CPPs could be used for the development of tracers for drug targeting, drug delivery, and molecular imaging. The present study compiles the serum stability, cellular uptake characteristics *in vitro* and *in vivo* and tumor uptake of ten frequently used CPPs. Although the field of CPPs attracted significant attention in a large number of studies,[33,34] little attention has been focused on the behavior of these peptides with respect to their *in vivo* accumulation specificity. The main objective of this study was to determine whether CPPs may be used as selective delivery vectors to target tumor tissue or organs such as the lungs, heart, liver, kidney, and spleen or even to cross the blood brain barrier. Most of the previous studies have been limited to the comparison of two or three peptides[35−37] and, as evaluated by Vives et al., concentrated on two peptides, Tat (presented in 44% of the studies) and penetratin (23% of the studies).[38] The aim of this work was to evaluate the *in vitro* and the *in vivo* properties of CPPs. This correlation requires data on a large series of different CPPs. In order to include CPPs from all major branches of the CPP family tree,[25] penetratin, Tat, $PreS_2$-TLM, MAP,

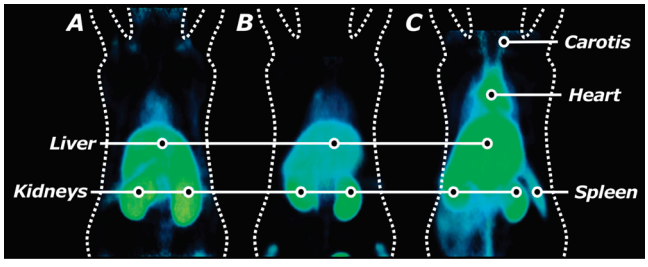

Figure 2. *In vivo* micro-PET imaging of the biodistribution of three labeled CPPs post intravenous injection. Wistar rats were injected with ^{68}Ga-labeled penetratin (A), Tat (B) and TP_{10} (C) via the tail vein and scanned at 1 h postinjection.

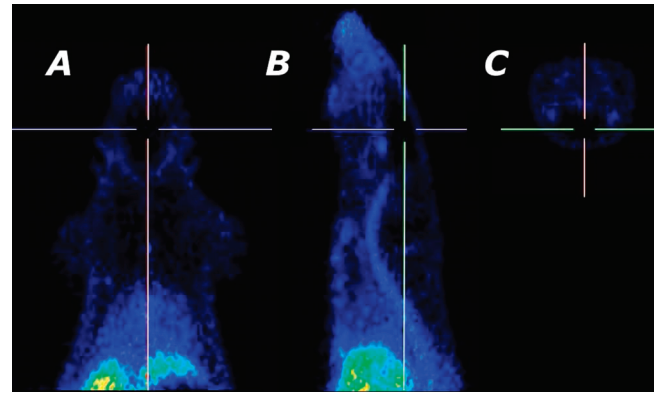

Figure 3. Brain image of a rat injected with ^{68}Ga-labeled Tat. The animal was scanned at 1 h post injection of the tracer via the tail vein. Crosshair is positioned on the brain. Axial (A), sagittal (B) and coronal (C) views are shown.

R_9, pVEC, MTS (K-FGF), $SynB_1$, $transportan_{10}$, and NLS (SV 40) were selected because these peptides represent the most frequently used CPPs.

Even though large cargoes have been shown to be transported by CPPs with little loss of transport capacity, the influence of the cargo on the peptide properties was a foremost consideration in the study design.[39] To minimize the influence exerted by the cargo (reporter group) on the pharmacokinetics, radiometal-labeled conjugates were selected using chelation by the macrocyclic chelator DOTA, which is known to provide an excellent *in vivo* stability.[40] In general, DOTA was placed at the *N*-terminus of the peptides. In the case of TP_{10} DOTA was placed at the ε-amino group of Lys at position 7 as described by Soomets et al.,[5] while in NLS DOTA at an additional lysine was placed at the *C*-terminus because it has been shown that modifications at this position do not influence the properties of NLS.[31] In contrast to the numerous studies conducted with fluorescent reporter groups (i.e., fluorescein isothiocyanate) this label enables a precise and uninfluenced quantification and provides the option of noninvasive imaging of the tracer accumulation.

The peptide half-lives in human serum were distributed over a wide range, with values from 1 to over 72 h (Table 1). Interestingly, penetratin, which undergoes the fastest degradation, and MAP, the most stable peptide, were at opposite edges of the stability values even though they represented the most efficient peptides in the *in vitro* study. The rapid degradation of R_9 (contains only RR bonds) reflects the low stability of the arginine−arginine bond. The fact that all of the CPPs containing at least one RR bond (Tat, $SynB_1$, pVEC, and penetratin) showed a faster degradation compared to the CPPs not containing an RR bond (MTS, TP_{10}, NLS, and MAP) shows that the RR bond represents a crucial factor for stability.

Hallbrink et al., who compared the cellular uptake of 4 different CPPs[41] *in vitro*, found that MAP had the highest efficiency, followed by $transportan_{10}$, Tat and penetratin respectively. In this study, the cellular uptake of penetratin was more efficient than the cellular uptake of Tat in all six cell lines used. On the whole, the CPPs studied revealed no specificity toward any of the tested cell lines.

The human prostate carcinoma PC-3 tumor was chosen as a tumor model to determine a possible tumor specific accumulation of one of the CPPs because the *in vitro* data revealed a time-dependent quite stable accumulation of 4 CPPs (penetratin, MAP, pVEC and $transportan_{10}$).

The study of the pharmacokinetics of all CPPs studied revealed a transient accumulation in the capillary-rich well-perfused organs liver, spleen, lung, and kidneys. The peptides showed a relatively fast blood clearance; the blood concentrations decreased to about 1 %ID/g (percentage of the injected dose/g) after 1 h and lower than 1 %ID/g after 4 h. None of the ^{111}In-CPPs demonstrated specificity toward the PC-3 tumor xenografts in athymic nude mice.

Even though CPPs can be used to facilitate the delivery of cargoes that varies greatly in size and nature, most of the applications describe the delivery of viral vectors,[42] macromolecular carriers,[17,19] proteins[43] and nucleic acids.[44] Tat and penetratin are established as the favorable choice for all kinds of cargoes; this convention omitted the potential value of other CPPs. Surprisingly, no preferences for CPP−cargo combination choices or the usage of an appropriate CPP to target a defined tissue or organ have been described. The data presented reveal that the CPPs are rapidly cleared and therefore do not show a pronounced tissue specificity. Consequently they may show their highest potential for topical applications and in combination with cargoes that dominate pharmacokinetic behavior. One possibility to improve the pharmacokinetics profile of CPPs could be to decrease their high clearance rate. This could be achieved by the attachment of CPPs to a macromolecular carrier (i.e., a nanoparticle or liposome) resulting in passive targeting via the enhanced permeability and retention (EPR) effect which

(33) Kersemans, V.; Cornelissen, B. Targeting the Tumour: Cell Penetrating Peptides for Molecular Imaging and Radiotherapy. *Pharmaceuticals* **2010**, *3*, 600–620.
(34) Kersemans, V.; Kersemans, K.; Cornelissen, B. Cell Penetrating Peptides for *in vivo* Molecular Imaging Applications. *Curr. Pharm. Des.* **2008**, *14*, 2415–2447.
(35) El-Andaloussi, S.; Jarver, P.; Johansson, H. J.; Langel, U. Cargo-Dependent Cytotoxicity and Delivery Efficacy of Cell-Penetrating Peptides: A Comparative Study. *Biochem. J.* **2007**, *407*, 285–292.
(36) Tacken, P. J.; Joosten, B.; Reddy, A.; Wu, D.; Eek, A.; Laverman, P.; Kretz-Rommel, A.; Adema, G. J.; Torensma, R.; Figdor, C. G. No Advantage of Cell-Penetrating Peptides over Receptor-Specific Antibodies in Targeting Antigen to Human Dendritic Cells for Cross-Presentation. *J. Immunol.* **2008**, *180*, 7687–7696.
(37) Neundorf, I.; Rennert, R.; Franke, J.; Közle, I.; Bergmann, R. Detailed Analysis Concerning the Biodistribution and Metabolism of Human Calcitonin-Derived Cell-Penetrating Peptides. *Bioconjugate Chem.* **2008**, *19*, 1596–1603.
(38) Vives, E. Present and Future of Cell-Penetrating Peptide Mediated Delivery Systems: "Is the Trojan Horse Too Wild to Go Only to Troy?" *J. Controlled Release* **2005**, *109*, 77–85.
(39) Schwarze, S. R.; Ho, A.; Vocero-Akbani, A.; Dowdy, S. F. *In vivo* Protein Transduction: Delivery of a Biologically Active Protein into the Mouse. *Science* **1999**, *285*, 1569–1572.
(40) Wadas, T. J.; Wong, E. H.; Weisman, G. R.; Anderson, C. J. Coordinating Radiometals of Copper, Gallium, Indium, Yttrium, and Zirconium for PET and SPECT Imaging of Disease. *Chem. Rev.* **2010**, *110*, 2858–2902.
(41) Hallbrink, M.; Floren, A.; Elmquist, A.; Pooga, M.; Bartfai, T.; Langel, U. Cargo Delivery Kinetics of Cell-Penetrating Peptides. *Biochim. Biophys. Acta* **2001**, *1515*, 101–109.
(42) Gratton, J. P.; Yu, J.; Griffith, J. W.; Babbitt, R. W.; Scotland, R. S.; Hickey, R.; Giordano, F. J.; Sessa, W. C. Cell-Permeable Peptides Improve Cellular Uptake and Therapeutic Gene Delivery of Replication-Deficient Viruses in Cells and *in vivo*. *Nat. Med.* **2003**, *9*, 357–362.
(43) Patel, L.; Zaro, J.; Shen, W.-C. Cell Penetrating Peptides: Intracellular Pathways and Pharmaceutical Perspectives. *Pharm. Res.* **2007**, *24*, 1977–1992.
(44) Juliano, R.; Alam, M. R.; Dixit, V.; Kang, H. Mechanisms and Strategies for Effective Delivery of Antisense and siRNA Oligonucleotides. *Nucleic Acids Res.* **2008**, *36*, 4158–4171.

is influenced by large molecules.[45−47] This approach should allow high targeting rates by the combination of the EPR effect combined with the internalization capacity of the CPPs. Similarly, the receptor-independent binding of viral vectors may be exploited using CPPs−virus conjugates because immune responses are an important drawback that limits the use of viral vectors to achieve acceptable gene expression.[48]

CPPs are considered to be able to cross the blood brain barrier, and several CPPs have been previously reported as efficient drug carriers to deliver many kind of cargoes to the brain through the blood brain barrier.[39,49,50] However, our findings show only moderate and transient uptake in the brain as the peak of accumulation, detected, did not exceed 1 %ID/g at 10 min p.i. The permeability of penetratin was 2−3-fold higher than the most frequently used Tat and $SynB_1$.

The brain uptake does not correlate with lipophilicity expressed as a grand average of hydropathicity (GRAVY):[51] the highest brain uptake values were observed for penetratin, Tat, and NLS, even though these peptides ranked among the most hydrophilic peptides. This reveals that the penetration of the blood brain barrier by the CPPs is a more complex or even a more specific process and not only an accumulation caused by the lipophilicity of the compounds.

The only significant value of MAP peptide, the most valuable peptide in the *in vitro* study, was its relatively slow blood clearance. The clearance from blood was not correlated with the lipophilicity expressed as grand average of hydropathy (GRAVY) values as MAP (the peptide with the slowest blood clearance) and MTS (the peptide with the fastest blood clearance) have the highest GRAVY values in this study indicating that clearance from blood of CPPs does not depend on the hydrophilic or hydrophobic properties.

As shown in Tables 3 and 4 (biodistribution data 10 min and 1 h after injection), the most important values of the biodistribution of penetratin and R_9 indicate that they are drug carriers to the spleen. The biodistribution of pVEC peptide revealed that its uptake is high in the liver (23.8 %ID/g) and low in the other organs (except the kidneys) after 4 h indicating that this peptide may be used as a drug carrier to the liver. Similar considerations apply to R_9. The NLS peptide showed a peak of accumulation in the kidneys 81.4 %ID/g, 94 %ID/g, and 88.3 %ID/g after 10 min, 1 h, and 4 h, respectively.

Three labeled CPPs were tested by small animal PET imaging, penetratin, Tat, and TP_{10}; the results observed in the biodistribution studies were confirmed by using these PET imaging studies. A rapid clearance from the blood and a distribution of these peptides in the well-perfused organs was observed (Figure 2). In the case of penetratin, major accumulation was observed in the spleen, the liver, and the kidneys. The highest fraction of Tat uptake was detected in the liver and the kidneys, while TP_{10} was distributed more broadly in the kidneys, liver, and spleen.

The biodistribution data have to be considered for the design of CPP conjugates. The high uptake rates observed *in vitro* and the relatively low specificity, combined with the fast clearance rates, implies that CPP-based delivery approaches may show their highest potential for topical applications. A further preferred application might be combined targeting strategies that involve a targeting step that is followed by the cellular uptake triggered by the CPP, for example viral transfections with an initial receptor-independent binding of virus to the plasma membrane.[52,53]

Conclusion

The pharmacokinetic properties of CPPs determined *in vitro*, *in vivo* and in the molecular imaging study could be helpful for the design and development of new radiopharmaceuticals and targeted pharmaceuticals in general. This information may facilitate the choice of CPPs depending on the delivery system and/or the molecule to be delivered, especially as it gives a prior vision about the biodistribution and the stability of the drug carrier used.

Acknowledgment. The authors thank Ursula Schierbaum for excellent technical assistance in the animal experiments. This work was supported by the Deutsche Forschungsgemeinschaft Grant Number HA 2901/6-1.

MP100223D

(45) Torchilin, V. P. Tatp-Mediated Intracellular Delivery of Pharmaceutical Nanocarriers. *Biochem. Soc. Trans.* **2007**, *35*, 816–820.
(46) Torchilin, V. P. Cell Penetrating Peptide-Modified Pharmaceutical Nanocarriers for Intracellular Drug and Gene Delivery. *Biopolymers* **2008**, *90*, 604–610.
(47) Christie, R. J.; Grainger, D. W. Design Strategies to Improve Soluble Macromolecular Delivery Constructs. *Adv. Drug Delivery Rev.* **2003**, *55*, 421–437.
(48) Baek, S.; March, K. L. Gene Therapy for Restenosis: Getting Nearer the Heart of the Matter. *Circ. Res.* **1998**, *82*, 295–305.
(49) Drin, G.; Rousselle, C.; Scherrmann, J. M.; Rees, A. R.; Temsamani, J. Peptide Delivery to the Brain via Adsorptive-Mediated Endocytosis: Advances with SynB Vectors. *AAPS PharmSciTech* **2002**, *4*, E26.
(50) Dietz, G. P. H.; Bähr, M. Peptide-Enhanced Cellular Internalization of Proteins in Neuroscience. *Brain Res. Bull.* **2005**, *68*, 103–114.
(51) Kyte, J.; Doolittle, R. F. A Simple Method for Displaying the Hydropathic Character of a Protein. *J. Mol. Biol.* **1982**, *157*, 105–132.
(52) Pizzato, M.; Marlow, S. A.; Blair, E. D.; Takeuchi, Y. Initial Binding of Murine Leukemia Virus Particles to Cells Does Not Require Specific Env-Receptor Interaction. *J. Virol.* **1999**, *73*, 8599–8611.
(53) Sharma, S.; Miyanohara, A.; Friedmann, T. Separable Mechanisms of Attachment and Cell Uptake during Retrovirus Infection. *J. Virol.* **2000**, *74*, 10790–10795.